Comparison of Short-Circuit Current Calculations in DC Shipboard Power System for Fuse's Protection Designing

J. J. Deroualle, D. Pescatori, A. Dellacasa, C. Davico

***Abstract*—In this article the protection design in a shipboard power system (SPS) with dc common bus distribution is evaluated. The goal is to compare two different approaches to calculate dc short-circuit currents and their outcoming influence in verifying the sensitivity of high-speed fuses. A dual fault analysis is proposed with time-domain simulation of a preponderant RLC circuit model, and the calculation procedures proposed by IEC 61660-1. Adequate study case is introduced considering a small innovative vessel powered by fuel cells and batteries with dc architecture for the electrical propulsion plant. The fault study is carried out considering the ship operations at Harbour with the minimum available power source. Finally, this paper highlights the benefits and limitations of the two dc fault methodologies and analyses their suitability for feeder protection designing with high-speed fuses in the dc SPS.**

***Keywords*: Shipboard power system (SPS), dc fault protection, high-speed fuses, sensitivity, dc fault current, IEC 61660-1.**

I. Introduction

SINCE the advent of the first ship powered with diesel-electric integrated propulsion *Queen Elizabeth* (1987), the power system distribution in ac has been the state-of-the-art in marine applications (all-electric ship) [1]. In the last decade, a variety of alternative power generations and distribution arrangements have been proposed for SPS [2]. Of these, the energy storage systems (ESS) have demanded for integration issues that are better addressed with the implementation of dc networks – with the elimination of reactive power and synchronization process the system becomes simpler in terms of designing and controlling [3]. It is also worthy to mention that the commercial marine applications are also seeking for fuel economy (variable-speed diesel generators can be easily integrated), while the navy is specially interested in suitable networks that can withstand high-power pulsed loads.

The improvements in power converters in terms of high currents and voltages supportability, together with dc static circuit breakers (capable of dealing with the non-current zero crossing), have rendered the dc SPS as a promising alternative to ac distribution for certain applications [4]. However, the lack of standards and guidance on the implementation of comprehensive short-circuit fault management within dc SPS has proved to be challenging in the design of such systems [2]. The challenges evolving fault detection and fault isolation are guided by the criticality of marine propulsion loads [2] together with the correct evaluation of short-circuit currents in the dc grid (those fault studies are of the most importance for understanding the aftermath of the fault [2] and selecting the appropriate protection for the network).

Even though simplified procedures for the dc short-circuit current calculation are documented in some papers and standards, these are not well established for SPS [5]. For instance, there is no IEEE guidance for the determination of dc fault levels for those systems [5]; the only document that is available on the subject is the IEC 61660-1 [5] (which is properly addressed to auxiliary installations in power plants and substations [6]). Therefore, a dynamic simulation – i.e. ATP version of the Electromagnetic Transients Program (EMTP) – is strongly advised to be carried out in order to complement the quasi-steady-state methods described by IEC 61660-1 [5].

The purpose of this paper is to investigate the short-circuit currents and its influence on the protection sizing in a Zero Emission Ultimate Ship (ZEUS) (Fig.1), which is a research boat equipped with a hybrid apparatus – 2 Diesel Generators (DGs) and 2 Propulsion Motors – to be used as a conventional propulsion system [7]. The main features includes 130 kW fuel cell system, powered by about 50 kg of hydrogen contained in 8 metal hydride cylinders; and a battery system, which united will allow an autonomy of about 8 hours of Zero Emissions navigation at a speed of 7.5 knots [7]. This document is divided into five sections. In Section II, the grid architecture of ZEUS and the corresponding electrical modeling are described. The principles of fault currents in dc SPS are addressed together with protection selectivity in Section III. Section IV deals with the comparison between IEC and dynamic simulations of dc fault currents and their influence on protection dimensioning. Section V summaries the results.

II. ZEUS DC SPS Modeling

ZEUS electrical propulsion plant has a common dc bus topology as described in [2]. This is an equivalent radial

ZEUS is part of the TecBIA research project conducted by Fincantieri S.P.A. and co-founded by MISE (Italian Ministry of Economic Development).

Jacques Julien Deroualle is with Project Eng. Dept., Fincantieri SI S.p.a, Trieste, TS 34123 Italy (e-mail: Jacques.Deroualle@fincantierisi.it).
David Pescatori is with Project Eng. Dept, Fincantieri SI S.p.a, Trieste, TS 34123 Italy (e-mail: David.Pescatori@fincantierisi.it).
Andrea Dellacasa is with Submarine Design Dept. (Navy), Fincantieri S.p.a, Genova, GE 16129 Italy (e-mail: Andrea.Dellacasa@fincantieri.it).
Christian Davico is with Submarine Design Dept. (Navy), Fincantieri S.p.a, Genova, GE 16129 Italy (email: Christian.Davico@fincantieri.it).

Paper submitted to the International Conference on Power Systems Transients (IPST2021) in Belo Horizonte, Brazil June 6-10, 2021.

distribution system where all the generation apparatus and loads are connected to the two Propulsion Switchboards (SWBDs) installed in the ship [2] (the schematic of this grid is shown in Fig. 2).

Fig. 1. Representation of ZEUS design hull [7].

Each Propulsion Switchboard has a Diesel Generator, a Fuel Cell system, two Batteries as energy sources, a Propulsion Motor, and a common ac Hotel Load as electrical loads. In addition, one Thruster motor and a Shore connection system are connected to one of the Propulsion Switchboards. The shunt capacitor installed in both SWBDs have the purpose of increasing the system stability [8]. Furthermore, these extra capacitance in the grid can assure that there is enough energy to operate the high-speed fuses in case there is a fault between the dc poles [8]. All the feeder branches of the SWBDs are protected by means of high-speed fuses. These protection apparatuses are conceived to protect semiconductors from short-circuits, ensuring fast opening and clearing, thus minimizing the thermal energy let-through that can jeopardize the entire power converter.

As per naval class registration requirements, the main design rule is to have redundancy in the generation, propulsion, and distribution system. This requirement is generally achieved with the said two independent SWBDs [1] and bus separation with the use of a bus-tie switch based on solid-state technology (10-40 μs) [8].

The architecture of the two switchboards will allow the vessel to be operated in different modes according to Table I:

TABLE I
SHIP OPERATING MODES (SOM) FOR ZEUS

Modes	Power Sources	Power Consumers
DG Navigation	2x DG // 2x Batteries	2x Prop. and Hotel Load
Zero Emission	Fuel Cell // 2x Batteries	2x Prop. and Hotel Load
Zero Noise	2x Batteries	2x Prop. and Hotel Load
Maneuvering	2x DG // 2x Batteries	Bow Thr. and Hotel Load
Harbour	Shore Connection	2x Batt. and Hotel Load

For the purposes of the present paper the equipment modelling will take into consideration only components that are present in SOM Harbour (as will be explained further on the text, this is the worst-case condition for the short-circuit considerations).

A. Propulsion Switchboards

The SWBDs are rated 640 Vdc (±10%) with two 60x5 *m*m cooper busbars (length equal to 2.6 meters). By applying the equations given in IEC 61660-1 for calculating the loop inductance per unit length (rectangular cross-section), resistance per unit length (55°C), and joint resistance; we obtain the following SWBDs parameters:

$$L' = \frac{\mu_o}{\pi}\left(\frac{3}{2} + \ln\frac{80\text{mm}}{60\text{mm} + 5\text{mm}}\right) = 0.6831\ {}^{\mu\text{H}}/_{\text{m}} \tag{1}$$

$$R'_{20} = 2\frac{{}^{1}/_{54}\ {}^{\Omega\text{mm}^2}/_{\text{m}}}{300\text{mm}^2} = 0.1235\ {}^{m\Omega}/_{\text{m}} \tag{2}$$

$$R'_{55} = R'_{20}[1 + 0.004\text{K}^{-1}(55°\text{C} - 20°\text{C})] \tag{3}$$

$$R_{joint} = 14\frac{{}^{1}/_{54}\ {}^{\Omega\text{mm}^2}/_{\text{m}}\ 60\text{mm}}{300\text{mm}^2} = 4.321\ \mu\Omega \tag{4}$$

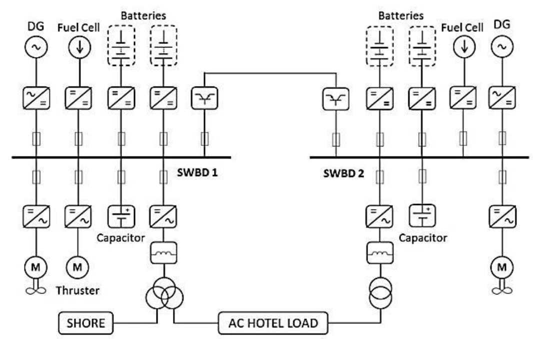

Fig. 2. ZEUS single line diagram (common dc bus topology).

The total loop inductance per SWBD is 1.776 μH, and the resistance referred to 55°C is 0.3659 $m\Omega$ (the SWBDs are dimensioned to operate until this rate of temperature). The dispositions of these parameters in the fault calculations followed the real physical arrangement made in the SWBDs.

B. Power Electronic Converters & Capacitors

As previously stated, only Harbour operating mode will be considered for the present paper. This imply that all power converters are connected to the dc grid in stand-by mode – there is only the fault contribution coming from the drivers' capacitors; exception made to ac Hotel Load circuit (described in the next point). The solid-state switches demand for current rise time limitation in the downstream section of the breaker, consequently a LC filter must be considered in the calculations. The LC filter used in the project has an inductance of 47 μH with a quality factor of 35.9 (50 Hz). In Table II all capacitor values used for the study are summarized. The capacitors were considered as being Metallized Polypropylene Film type (typical in dc-link applications with low values of ESL and ESR). The schematic used in the simulations for the dc bus (SWBD 1) is shown in Fig. 3.

C. AC Shore Connection

At the Harbour the shore connection will be responsible for supplying the ac loads and eventually charging the batteries. Considering the worst condition in terms of minimum short-circuit current, the batteries will be discharged, and unable to contribute to the fault current (only the capacitors of the related DC/DC drivers are present in the modeling of Fig. 3).

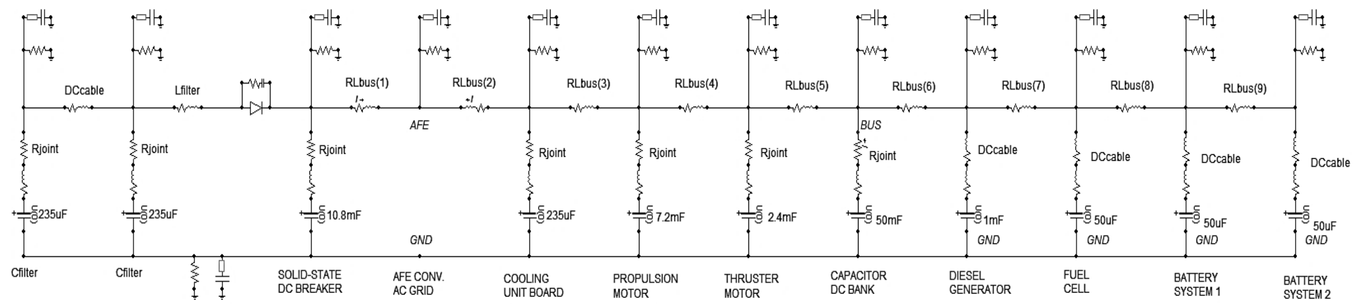

Fig. 3. ATP model of the dc-link in the SWBD 1 used for the simulations.

The only source that will effectively contribute to a possible short-circuit, in this case, is indeed the ac shore connection (Fig. 4).

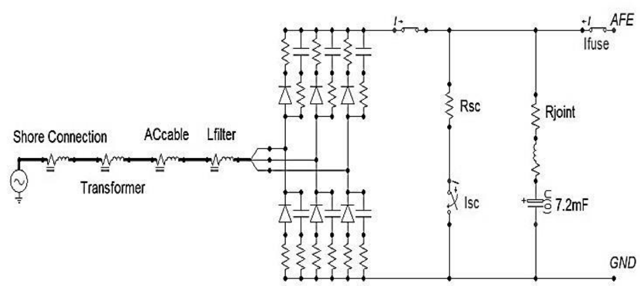

Fig. 4. ATP model of the shore connection converter in fault condition.

TABLE II
SYSTEM CAPACITOR PARAMETERS USED FOR THE STUDY

Converter	**Type**	**Capacitor [μF]**	**ESR [$m\Omega$]**	**ESL [nH]**
Propulsion	AC/DC	7,200.0	0.20	30.0
Thruster	AC/DC	2,400.0	0.05	30.0
AC Hotel Load	AC/DC	7,200.0	0.20	30.0
DG	AC/DC	1,000.0	0.05	30.0
Fuel Cell	DC/DC	50.0	0.01	30.0
Battery	DC/DC	50.0	0.01	30.0
DC Solid-State	Breaker	10,800.0	0.18	30.0
LC Filter	dv/dt	235.0	0.01	30.0
Board Shunt	Capacitor	50,000.0	0.05	30.0

As it can be seen in Fig. 2, the shore connection is connected to grid through a three winding (3W) transformer, which permits to feed at the same time the Propulsion SWBDs and ac Hotel Load. There is also an LC filter between the AFE converter and the primary winding, which limits together with the transformer the fault contribution coming from the shore connection (120 kA with an X/R of 4.0). The data from the transformer and filter is disposed in Table III.

In Fig. 4 all the impedances were reflected to the primary winding side (330 Vrms). The delta capacitance (47 μF) in the filter was neglected in the simulations.

A. Power Cables

The converters of the Diesel Generator, the Fuel Cell System and the Batteries are not contemplated inside the Propulsion SWBDs; they are connected to the dc bus using armoured power cables with improved EMC screening for the dc 0.9/1.5 kV. The two Propulsion are interconnected though a tie cable, as per static switch manufacturer recommendation: a four-core symmetrical shielded cable with maximum stray inductance of 500 nH. Variable frequency screening 1.8/3.0 kV cables was used for the connection of the transformer to the Propulsion SWBD.

TABLE III
SYSTEM TRANSFORMER AND FILTER PARAMETERS USED FOR THE STUDY

Equip.	**Rating**	**Voltage [Vrms]**	**Z%**	**X/R**
Transformer	65 kVA	330/400/400	4.5/4.5/7.0	3.5
LC Filter	155 A (50°C)	330	0.43 mH	21.9

III. FAULT CURRENTS IN DC SPS

The main effort of the protection coordination in the dc SPS originates from the low thermal capability of power converters based on semiconductors [8] associated with the fast discharging characteristics of capacitors (time range of few milliseconds). According to [2], considering the 2-level Voltage Source inverters (2L-VSC) in Fig. 2, the fault currents on the dc SPS are characterized by two responses: one is the transient discharge current from the dc-link capacitors, and the other is the steady-state current supplied by the generating sources (the motors will contribute for just a short period of time). This high-capacitive discharge current is only limited by a low busbar impedance, therefore reflecting in an oscillating transient current curve (underdamped condition).

A. ZEUS Protection Selectivity and Sensitivity

When the short-circuit occurs in any section of the SWBDs, the dc solid-state breaker in the interconnector branch will open almost instantaneously, isolating the faulty board and allowing the continuity of service. The fuses in the isolated board will be responsible for extinguish the fault, so it has to be assured that the fault energy provided from the capacitors is sufficient to achieve the fuse's melting point in proper time (sensitivity). In this case, it is not of major concern the achievement of selectivity between the feeders (it is expected the operation of more than one feeder's fuse).

In case that the dc static breaker fails to interrupt, all loads in the healthy SWBD experiment a fast drop voltage and may be disconnected due to the driver's undervoltage protection, resulting in a total black-out for the system [8].

There is a trade-off in terms of protection sensitivity and the peak fault current. Higher values of capacitance in the dc system, besides supporting the system stability [8], ensures that in all SOMs there will be fault current for melting the fuses, but at the same time it will increase the fault peak level and, consequently, the transient oscillations. So, a faulty study is of most significant importance for investigating the fault conditions scenarios in the dc SPS and the suitable schemes of electrical protection.

B. High-Speed Fuses Performance Valuation

Most converter manufacturers give the joule integral ratings (i^2t) that should not be exceeded for their product in a period below 10 *m*s. In some cases, it is also suggested the fuses ratings to be used in the datasheets (but remaining to the grid's designer the responsibility in checking the clearing times and its efficacy in the network). The electrical characteristics of fuses that was considered for ZEUS project are shown in Table IV.

TABLE IV
SYSTEM HIGH-SPEED FUSES PARAMETERS USED FOR THE STUDY
(THE CLEARING ENERGY IS REFERRED TO AC VOLTAGES)

Converter	Fuse Class	In [A]	Pre-arc [A^2s]	Clearing [A^2s]
AC Hotel Load	aR	400.0	15,000.0	105,000.0 (660V)
Thruster	aR	200.0	2,200.0	15,000.0 (660V)
Propulsion	aR	400.0	15,000.0	105,000.0 (660V)
DG	gR	550.0	100,000.0	515,000.0 (600V)
Fuel Cell	gR	250.0	10,000.0	52,500.0 (600V)
Battery	gR	250.0	10,000.0	52,500.0 (600V)
DC Breaker	aR	800.0	69,500.0	465,000.0 (660V)

The protection fault study should be conducted minding the minimum short-circuit current that can manifest in the grid. When calculating these currents, according to [6], the follow conditions should be observed: the conductor resistances are referred to the maximum operating temperature; joint resistances must be taken into consideration, the batteries are at final voltage (or even discharged); any diode for decoupling parts of the system is taken into account; the current limiting effect of protection devices is to be considered (dc static breakers are opened).

One possible way to analyze the fuse's melting time in the minimum fault current condition is to plot in the same graph the rms current values of the prospective short-circuit (5) and the fuse's melting and clearing curves – that are ruled by the joule integral values in the first 10 *m*s of fault (this method was also proposed in [8]). The effectiveness of the protection is confirmed when the current curve crosses the melting curves – the clearing times informed in Table IV are referred to 660 and 600 Vac (IEC). ZEUS dc SPS is nominally rated 640 Vdc, which brings some uncertainty in the clearing time (mitigated by the time window of 10 *m*s).

$$i_{rms}(t_1) = \sqrt{\frac{\int_0^{t_1} i^2(t)dt}{t_1}} \quad (5)$$

IV. EXAMPLE AND STUDY FAULT'S APPLICABILITY

To demonstrate the effect in dimensioning the high-speed fuses, the fault study example (and comparison between dynamic simulations and IEC 61660-1 calculation procedures) has considered the Harbour system condition; in order to get the minimum short-circuit conditions.

The equivalent circuit in such fault topology is shown in Fig. 5. The example will be based in a fault event in the ac Hotel Load converter feeder, where the batteries are completely discharged, the busbar voltage are at 90% of the nominal value (576 Vdc), and the tie-breaker section will open instantaneously, leading to a circuit model in which only the capacitors from SWBD 1 are contributing to the prospective short-circuit current (and also the capacitor in the LC filter of SWBD 2). In this case the only power source that is feeding the fault circuit is the 400 Vrms shore-connection through the 3W transformer.

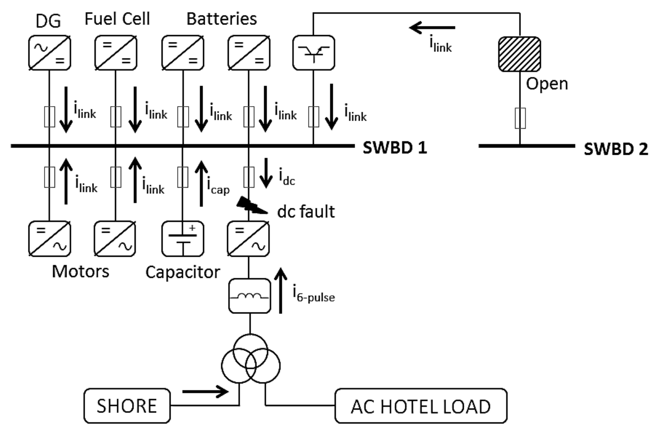

Fig. 5. Fault current flows on SOM Harbour.

The nominal current of the fuse located in ac Hotel Load feeder is 400 Arms (Table IV). The fault study must verify that in such poor conditions there will be enough energy to blow-up the aR type fuse in due time.

A. IEC Short-Circuit Current Calculations

The total short-circuit current at the fault point is obtained by the superposition principle of the individual branch short-circuit currents from the different equipment. Moreover, when there is a common branch in the circulating fault currents, the partial short-circuit currents of the different sources are to be corrected with factors σ_j, which derives from the different resistance's sources and from the common branches. In this analysis only two types of dc sources are considered: converters in a three-phase bridge configuration, and dc-link capacitors.

Generally speaking, the fault current is described by a time function $i_1(t)$, where t_p is the time to achieve the initial peak current (i_p); and a second function $i_2(t)$ representing the decaying time until the achievement of the quasi steady-state current I_k as outlined in (7).

The following definitions apply: T_k is the short-circuit duration, the rise time constant is represented by τ_1; and the decay time constant by τ_2.

$$i_1(t) = i_p \frac{1 - e^{-t/\tau_1}}{1 - e^{-t_p/\tau_1}} \quad \text{for } 0 \le t \le t_p \tag{6}$$

$$i_2(t) = i_p \left[\left(1 - \frac{I_k}{i_p}\right) e^{-(t-t_p)/\tau_2} + \frac{I_k}{i_p} \right] \quad \text{for } t \ge t_p \tag{7}$$

The current parameters obtained for the study case in Fig. 5 are displayed in the Table V. The fault calculations considered the electrical circuits from Fig. 3-4, divided into smooth capacitors and converter rectifier constants. Following the recommendations of [9], the correction factors σ_j are not applicable to the resistances of capacitors up to the common branch (AFE converter from the ac Hotel Load).

TABLE V
IEC STANDARD SHORT-CIRCUIT CURRENTS
CONTRIBUTION FROM EACH INDIVIDUAL BRANCH EQUIPMENT

Branch	**I_k [kA]**	**I_p [kA]**	**t_p [ms]**	**τ_1 [ms]**	**τ_2 [ms]**
Battery Cap. 1	0.0	3.66	0.035	0.021	0.031
Battery Cap. 2	0.0	3.65	0.035	0.021	0.032
Fuel Cell Cap.2	0.0	2.94	0.035	0.021	0.031
DG Cap.	0.0	10.18	0.13	0.075	0.226
Capacitor Bank	0.0	116.38	0.35	0.182	0.495
Thruster Cap.	0.0	48.34	0.07	0.041	0.086
Propulsion Cap.	0.0	80.01	0.075	0.041	0.093
Cooling Unit Cap.	0.0	21.74	0.018	0.011	0.012
C Filter SWBD 1	0.0	7.60	0.18	0.108	0.214
C Filter SWBD 2	0.0	1.88	0.18	0.104	0.144
dc Breaker Cap.	0.0	90.30	0.12	0.065	0.11
AC Load Cap.	0.0	143.48	0.02	0.01	0.043
6-pulse Rectifier	1.588	2.67	11.04	3.95	21.134

B. Standard and Time-Domain Simulation Analogies

The proposed fault study comparison for time-domain circuit simulation and IEC 61660-1 procedures is shown in Fig. 6. The conclusions made in [6], noticing that current values obtained by IEC methodology are larger than the corresponding values of the transient analysis, can be also observed for the ZEUS dc SPS. The main implications are that the standard provides conservative results and doesn't consider the underdamping transient curves.

The typical current-time for the 6-pulse rectifier is also seen in Fig. 6 (a). The peak at half-cycle is due to the same reason that creates a dc offset in ac fault calculations [5]. The magnitude of this peak is mainly affected by the X/R ratio [5].

Another implication from the curves in Fig. 6 is that the fault current from the converter can be neglected in the protection fault study analysis. The proposed RLC equivalent circuit model in [8] is sufficient for determining the high-speed fuse's effectiveness – the fault current contribution from ac generators, motors, and shore-connection, is much lower and with a higher rising time constant than that of the dc-link capacitors [8].

The total short-circuit at the fault point (capacitors and rectifier contributions superposed) is displayed in Fig. 7.

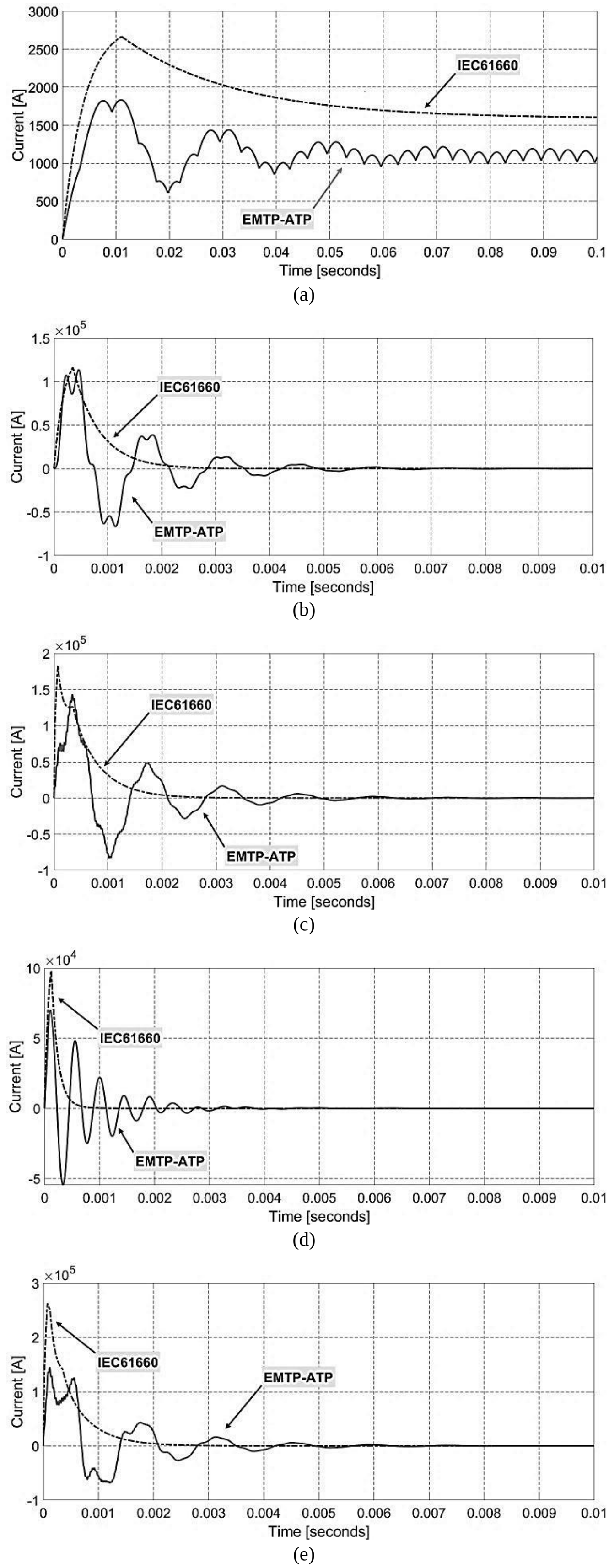

Fig. 6. Prospective short-circuit currents of ATP simulation (solid line) and IEC 61660-1 (dashed line). (a) Rectifier Converter. (b) Capacitor bank in the dc-link. (c) SWBD right-side from the fault point. (d) SWBD left-side from the fault point. (e) SWBD total contribution (fault current passing through 400 A high-speed fuse).

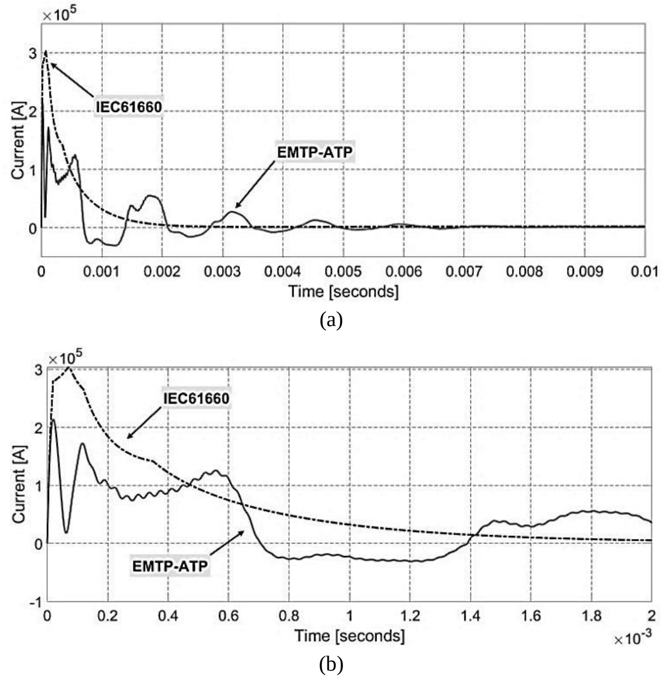

Fig. 7. Total short-circuit current at the fault point of ATP simulation (solid line) and IEC 61660-1 (dashed line). (a) 10 *m*s time interval. (b) 2 *m*s time interval.

It is again noticeable that the capacitor's fault current plays a major role in the first 10 *m*s of transients. Another characteristic of fault currents in dc SPS is the low value in the steady-state term, which means that the SWBDs are rated for higher values of peak current and lower thermal ones.

C. Sensitivity Analyzes of the High-Speed Fuses

The joule integral of the total short-circuit currents is presented in Fig. 8. The higher value of energy associated with the standard results is a consequence of IEC conservative methodology – in the specific case of dc SPS, there is a clear suggestion that the use of correction factors for common branches associated with capacitors would bring a more realistic outcome.

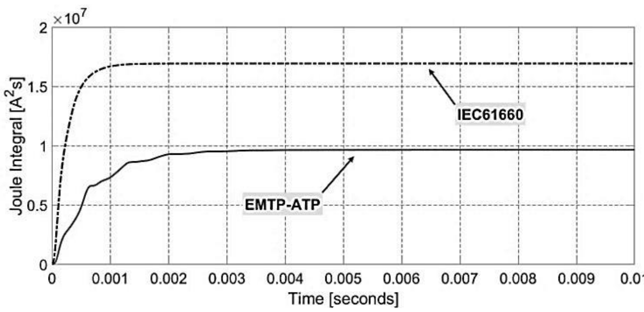

Fig. 8. Joule Integral of the correspondent total short-circuit currents.

In Fig. 9 it is exposed the sensitivity analysis for the 400 A high speed fuse. Both calculation methods confirmed the clearing time in less than 1 *m*s, demonstrating the effectiveness of the chosen protection component by the manufacturer. For the scope of the present example, the standard proved to be suitable to confirm the fuse's clearing (it is recommended that in case the IEC procedure is used, to downgrade the fuse's current if the fuse melting region is located next to the calculated rms peak current).

Nevertheless, if the focus of the fault study is to confirm the selectivity protection between the feeders – just like the ABC method proposed in [8] – the IEC is not indicated, requiring precise results that are offered by transient dynamic simulations.

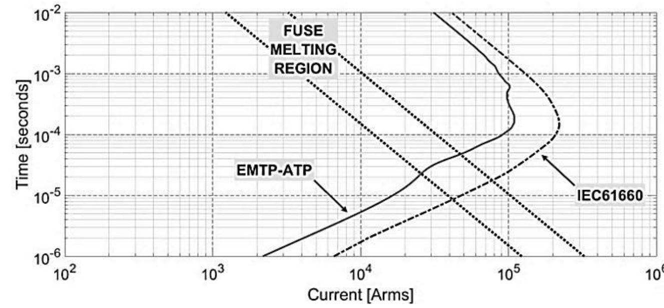

Fig. 9. Sensitivity analyses for ac Hotel Load branch from ZEUS dc SPS.

V. Conclusions

This paper proposed the comparison of two methodologies for calculating the dc fault currents and their implications in the protection's check designing of a Zero Emission ship. Both fault studies proved to be reliable regarding the sensitivity analysis that involves high-speed fuses. Due to the transient simplifications (correction factors are neglected for capacitors containing common branch circuits) and conservative procedures adopted for the IEC, the selectivity analysis should be better addressed by time-domain transient simulations. The dc SPS can be modelled for such protection studies as simplified RLC equivalent circuits.

VI. References

[1] E. Haugan, H. Rygg, A. Skjellnes and L. Barstad, "Discrimination in Offshore and Marine DC Distribution Systems," 2016 IEEE 17th Workshop on Control and Modeling for Power Electronics (COMPEL), Trondheim, 2016, pp. 1-7.

[2] K. Satpathi, A. Ukil and J. Pou, "Short-Circuit Fault Management in DC Electric Ship Propulsion System: Protection Requirements, Review of Existing Technologies and Future Research Trends," in IEEE Transactions on Transportation Electrification, vol. 4, no. 1, pp. 272-291, March 2018.

[3] Z. Jin, G. Sulligoi, R. Cuzner, L. Meng, J. C. Vasquez and J. M. Guerrero, "Next-Generation Shipboard DC Power System: Introduction Smart Grid and dc Microgrid Technologies into Maritime Electrical Networks," in IEEE Electrification Magazine, vol. 4, no. 2, pp. 45-57, June 2016.

[4] A. Vicenzutti, E. De Din and G. Sulligoi, "Transient Short Circuit Analysis in DC on-board distribution systems fed by synchronous generators through 6-pulse diode rectifiers," 2015 International Conference on Electrical Systems for Aircraft, Railway, Ship Propulsion and Road Vehicles (ESARS), Aachen, 2015, pp. 1-6.

[5] J. C. Das, "Arc Flash Hazard Calculations in LV and MV DC Systems - Part I: Short-Circuit Calculations," Conference Record of 2013 Annual IEEE Pulp and Paper Industry Technical Conference (PPIC), Charlotte, NC, 2013, pp. 81-92.

[6] A. Berizzi, A. Silvestri, D. Zaninelli and S. Massucco, "Short-Circuit Current Calculations for DC Systems," in IEEE Transactions on Industry Applications, vol. 32, no. 5, pp. 990-997, Sept.-Oct. 1996.

[7] G. Scagnetti, "Fincantieri, ricerca e sperimentazioni: impostata unita sperimentale ZEUS." Insidertrend Magazine, September 23, 2020. https://www.insidertrend.it/2020/09/23/energia/industria-navale-fincantieri-ricerca-e-sperimentazioni-impostata-unita-sperimentale-zeus/

[8] S. Kim, S. Kim and D. Dujic, "Extending Protection Selectivity in DC Shipboard Power Systems by Means of Additional Bus Capacitance," in IEEE Transactions on Industrial Electronics, vol. 67, no. 5, pp. 3673-3683, May 2020.

[9] *Short-Circuit Currents in DC Auxiliary Installations in Power Plants and Substations*, IEC Standard 61660-1, 1997.